2023-02-14

Differences in toxicity and accumulation of metal from copper oxide nanomaterials compared to copper sulphate in zebrafish embryos: Delayed hatching, the chorion barrier and physiological effects

Pereira, SPP

10.1016/j.ecoenv.2023.114613
Ecotoxicology and Environmental Safety
Elsevier BV

Ecotoxicology and Environmental Safety 253 (2023) 114613

Contents lists available at ScienceDirect

Ecotoxicology and Environmental Safety

journal homepage: www.elsevier.com/locate/ecoenv

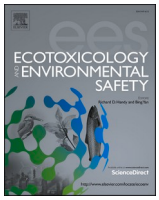

Differences in toxicity and accumulation of metal from copper oxide nanomaterials compared to copper sulphate in zebrafish embryos: Delayed hatching, the chorion barrier and physiological effects

Susana P.P. Pereira [a,b], David Boyle [b], António Nogueira [a], Richard D. Handy [b,*]

[a] Departamento de Biologia & CESAM, Universidade de Aveiro, 3810-193 Aveiro, Portugal
[b] School of Biological and Marine Sciences, University of Plymouth, Drake Circus, Plymouth, Devon PL4 8AA, UK

ARTICLE INFO

Edited by Professor Bing Yan

Keywords:
Danio rerio
Copper toxicity
Nanoparticles
Hatching inhibition
Ionic regulation
Glutathione

ABSTRACT

The mechanisms of toxicity of engineered nanomaterials (ENMs) to the early life stages of freshwater fish, and the relative hazard compared to dissolved metals, is only partially understood. In the present study, zebrafish embryos were exposed to lethal concentrations of copper sulphate ($CuSO_4$) or copper oxide (CuO) ENMs (primary size ~15 nm), and then the sub-lethal effects investigated at the LC_{10} concentrations over 96 h. The 96 h-LC_{50} (mean ± 95% CI) for $CuSO_4$ was 303 ± 14 μg Cu L^{-1} compared to 53 ± 9.9 mg L^{-1} of the whole material for CuO ENMs; with the ENMs being orders of magnitude less toxic than the metal salt. The EC_{50} for hatching success was 76 ± 11 μg Cu L^{-1} and 0.34 ± 0.78 mg L^{-1} for $CuSO_4$ and CuO ENMs respectively. Failure to hatch was associated with bubbles and foam-looking perivitelline fluid ($CuSO_4$), or particulate material smothering the chorion (CuO ENMs). In the sub-lethal exposures, about 42% of the total Cu as $CuSO_4$ was internalised, as measured by Cu accumulation in the de-chorionated embryos, but for the ENMs exposures, nearly all (94%) of the total Cu was associated with chorion; indicating the chorion as an effective barrier to protect the embryo from the ENMs in the short term. Both forms of Cu exposure caused sodium (Na^+) and calcium (Ca^{2+}), but not magnesium (Mg^{2+}), depletion from the embryos; and $CuSO_4$ caused some inhibition of the sodium pump (Na^+/K^+-ATPase) activity. Both forms of Cu exposure caused some loss of total glutathione (tGSH) in the embryos, but without induction of superoxide dismutase (SOD) activity. In conclusion, $CuSO_4$ was much more toxic than CuO ENMs to early life stage zebrafish, but there are subtle differences in the exposure and toxic mechanisms for each substance.

1. Introduction

Metal oxide nanomaterials are finding diverse industrial applications due to their unique physico-chemical properties at the nano scale. Copper oxide engineered nanomaterials (CuO ENMs) have applications as catalysts, in air and liquid filtration units, in wood preservatives and antifouling paints for boats, as well as in industrial sealants and coatings. CuO ENMs had a global annual production of 570 tons in 2014 and it is estimated to increase to 1600 tons by 2025 (Keller et al., 2013). About 5.5% of the manufacturing and domestic wastes from CuO ENMs are expected to reach natural water bodies (Keller et al., 2013); with some direct releases from some products (e.g., Cu ions from antifouling paints). Although the concentrations of Cu-containing ENMs in surface waters have not been determined, metal-containing ENMs are expected in the low μg L^{-1} to ng L^{-1} range (Lead et al., 2018). The fate and behaviour of CuO ENMs in freshwater ecosystems is only partially understood, but they show colloidal behaviours such as aggregation, dissolution, and flocculation (Amde et al., 2017; Ross and Knightes, 2022).

The dissolution of Cu-containing ENMs is a particular concern, as dissolved Cu is toxic to aquatic organisms in freshwater and with acutely lethal concentrations for fish around 10–150 μg L^{-1}, depending on the water sodium concentration, hardness and pH [reviews (Grosell et al., 2002; Handy, 2003)]. There is also the possibility that metal-containing ENMs could act as a delivery vehicle to release high concentrations of metals in the gill microenvironment of fishes (Shaw and Handy, 2011)

* Corresponding author.
E-mail addresses: susanapinper@gmail.com (S.P.P. Pereira), david.boyle@plymouth.ac.uk (D. Boyle), antonio.nogueira@ua.pt (A. Nogueira), R.Handy@plymouth.ac.uk (R.D. Handy).

https://doi.org/10.1016/j.ecoenv.2023.114613
Received 23 November 2022; Received in revised form 1 February 2023; Accepted 3 February 2023
Available online 14 February 2023

and Cu ENMs are toxic to fishes [rainbow trout, Shaw et al. (2012); zebrafish, Griffitt et al. (2007)]. The mode of action of dissolved Cu during waterborne exposure of freshwater fish is well-known and includes gill injury with a specific interference with sodium homeostasis and inhibition of the branchial sodium pump [the Na^+/K^+ ATPase (Grosell, 2011)]. Copper can also catalyse the Haber-Weiss reaction leading to oxygen radicals; and oxidative stress is also a feature of Cu toxicity to fishes (Eyckmans et al., 2011; Hoyle et al., 2007). These modes of actions also occur during exposure to Cu ENMs (e.g., Al-Bairuty et al., 2016; Malhotra et al., 2020; Shaw et al., 2012).

The early life stages of fishes are especially vulnerable to metal toxicity, including dissolved Cu in trout (McKim et al., 1978) and in zebrafish (Johnson et al., 2007). Evidence is also emerging of hazard from Cu-containing ENMs, at least to zebrafish larvae (McNeil et al., 2014). The early-life stages of zebrafish are now widely used in regulatory toxicity testing, most notably the fish embryo test (FET) OECD TG 236 (OECD, 2013), which has been validated for traditional chemicals (Busquet et al., 2014), but requires modifications to work for ENMs (Shaw et al., 2016). The sensitivity of zebrafish embryos to dissolved metals is influenced by the presence of the semi-permeable chorion and the ion-exchange properties of the mucous perivitelline fluid which is rich in fixed anionic residues to buffer metal uptake (Peterson & Martin-Robichaud, 1986; Shephard, 1987). After hatching, without the protection of the egg, the larvae are often more vulnerable to waterborne chemicals (Ganesan et al., 2016), and this is also the case with some ENMs (Shaw et al., 2016). Hatching success is often used as an endpoint in early life stage studies, and dissolved Cu has been shown to inhibit hatching with consequent impairment of embryos survival (Johnson et al., 2007; Zhang et al., 2018). Hatching occurs by the joint action of proteolytic enzymes (particularly ZHE_1) that are released in the perivitelline space (Muller et al., 2015) and the movements of the fish embryo to break the weakening chorion (Ong et al., 2014). Still, the mechanisms of action of CuO ENMs in zebrafish embryos, and whether the chorion is protective against ENMs remains unclear. Additionally, the differences in the internalization of ENMs and metal salt forms are not fully understood.

This study aimed to evaluate the lethal and sub-lethal effects of CuO ENMs in zebrafish embryos compare to that of $CuSO_4$. Mortality and hatching success were used as the endpoints to assess lethal effects on zebrafish embryos. To understand if chorion has a protective effect, experiments were conducted on embryos with the chorion present (chorionated) and without it (de-chorionated) and the subsequent metal accumulation and distribution in the embryos was measured. Finally, in de-chorionated embryos where internal Cu exposure was confirmed, the sub-lethal effects on osmoregulation [electrolyte concentrations and sodium pump (Na^+/K^+-ATPase activity)] and oxidative stress parameters [superoxide dismutase (SOD) activity and total glutathione (tGSH)] were measured to help unravel the mechanisms of toxicity of CuO ENMs.

2. Materials and methods

2.1. Copper oxide nanomaterials and characterisation

Copper oxide nanomaterials (uncoated, dry powder form, > 99% purity and expected average size of 30–50 nm) were obtained from PlasmaChem GmbH (Berlin, Germany). Stock suspensions of CuO ENMs (1 g L^{-1}) were prepared in ultrapure water (18 MΩ, ELGA DV25 Pure Lab Option-Q, Veolia Water Technologies, High Wycombe, UK) and dispersed by sonication for 1 h (160 W/L at 37 kHz; S-Series unheated ultrasonic cleaning bath, Fisherbrand, Loughborough, UK) before further dilutions in freshwater (aerated, dechlorinated and recirculating Plymouth city water). Stock solutions of 20 mg L^{-1} of Cu metal as $CuSO_4$ were prepared similarly to the CuO ENMs. The primary particle diameter and morphology of CuO ENMs was determined using a tomography electronic microscope (TEM, JEOL 12000EXII, Tokyo, Japan). Fresh (0 h) and aged (24 h) suspensions (50 g L^{-1}) of the CuO ENMs were prepared in both ultrapure water and tap water (freshwater) and measurements were made on triplicated samples. Small volumes (≈ 1 mL) of the suspensions were placed on the grids (copper coated with Formvar/carbon), allowed to sit for 10 min and then placed in the instrument for analysis. The primary particle diameters were measured on the images obtained using Image J (https://imagej.nih.gov/ij/) with at least 35 particles counted from each dispersion.

The suspensions of CuO ENMs were also examined for particle aggregation and settling behaviour over 24 h. Freshly prepared suspensions of CuO ENMs (25 mg L^{-1} of CuO ENMs in freshwater) were placed in triplicates (300 mL beakers previously acid washed and deionized) at room temperature without stirring and water samples taken after 0, 0.5, 1, 2, 4, 8, 24 h. From these suspensions, particle settling was estimated based on the loss of total copper concentrations from the water column over 24 h. Total metal concentrations were measured by inductively coupled plasm optical emission spectrometry (ICP-OES, Varian 725 ES, Agilent, Stockport, UK). Particle size distribution of the CuO ENMs (hydrodynamic diameters) was also evaluated in triplicate at the start and end of the same experiment using Nanoparticle Tracking Analysis (NTA, Nanosight LM10, Amesbury, UK).

Dissolution of dissolved Cu from the CuO ENMs was determined by equilibrium dialysis following the method of Besinis et al. (2014). These experiments were conducted in triplicate at room temperature using Plymouth water. All glassware was acid washed in 5% nitric acid and triple rinsed in ultrapure water before use (i.e., clean glassware not pre-equilibrated with the test solutions). The cellulose dialysis tubing [12 kDa molecular weight cut off (Sigma-Aldrich, Gillingham, UK)] were cut into strips (70 × 25 mm), thoroughly cleaned, acid washed and rinsed in ultrapure water. The dialysis bags were filled with either 3 mL of 2.5 g L^{-1} of CuO ENMs suspension (i.e., 7.5 mg of CuO ENMs in ultrapure water) or $CuSO_4$ solution (29.5 mg of $CuSO_4$ in ultrapure water) and then closed at both ends with Medi-clips to prevent leakages. The dialysis membranes were sealed, added to the beakers containing 297 mL of freshwater (the same composition as used for the fish) and stirred gently with a magnetic stirrer. Samples from the beakers (i.e., from outside the dialysis bag) were collected after 0, 0.5, 1, 2, 4, 8, 24 h and acidified (68% HNO_3) prior to total Cu determination by ICP-OES.

2.2. Experimental fish

Stocks of adult zebrafish (*Danio rerio*), bred in house at Plymouth University (Devon, UK) were held in a facility at 26 ± 1 ºC and 16 h light:8 h dark cycle. Fish were held in glass tanks (25 L) with aerated, recirculating, filtered and dechlorinated freshwater (water chemistry in mM, means ± S.D., n = 3: Ca^{2+}, 1.12 ± 0.05; K^+, 0.10 ± 0.01; Mg^{2+}, 0.14 ± 0.01; Na^+, 0.93 ± 0.04; pH 7.3; conductivity 168.3 μS/cm) (Boyle et al., 2020). The background concentration of Cu in the tap water was below the detection limit (LOD = 1.82 μg L^{-1}, n = *3* replicates). Fish were fed twice each day with flake and brine shrimp nauplii *ad libitum*. Breeding pairs of fish were allowed to spawn at first light and resulting embryos carefully collected into clean freshwater. Fertilized embryos in blastula stage (3–6 hpf) were selected for viability under a stereo microscope (Olympus SZX7 with an Infinity 2 camera, Tokyo, Japan) and separated from unfertilized eggs. Coagulated (white and opaque) or unhealthy embryos were discarded, and the batches of healthy embryos were kept in petri dishes prior exposure.

2.3. Lethal and sub-lethal exposures of zebrafish embryos

The embryo assay was based on the OECD Test Guideline no. 236 on Fish Embryo Toxicity Test (FET) (OECD, 2013). The tap water used for all egg collection procedures and toxicity assays was previously filtered (0.2 μm PES vacuum filter, VWR, Lutterworth, UK). Preliminary range finding experiments were performed to determine the lethal concentration of the CuO ENMs compared to $CuSO_4$, and to derive an LC_{10} for subsequent sub-lethal studies. A series of twelve concentrations (3

replicate plates, with a total of $n = 24$ replicate wells per concentration) in 48-well microplates (one embryo per well with 1 mL of exposure solution) was used for the lethality test. Endpoints were selected to assess acute lethality of both $CuSO_4$ and CuO ENMs, including % mortality (visually, opaque embryos were counted as dead) and % hatching success (visually, embryos able to break chorion). In addition, observations were made on 'perivitelline fluid morphology' that represents embryos with an abnormal perivitelline fluid (appearance of bubbles and foam-looking that is not present in the control), and "surface coated chorion" that represents the proportion of embryos with chorion visually coated with ENMs. After determining the lethal concentration that killed 10% of embryos (LC_{10}) values (see supplementary information), sub-lethal assays were performed with 20 mg L^{-1} of CuO ENMs and 190 μg L^{-1} of Cu as $CuSO_4$. Exposures were conducted in low-density polypropylene cups (100 embryos in 100 mL of Cu suspensions) with triplicates per treatment and an unexposed control for reference. All assays were incubated at 26 ± 1 ºC and 16 h light/8 h dark cycle for 96 h. Suspensions of CuO ENMs and solutions of $CuSO_4$ were renewed daily (after 24 h) to maintain the exposures. After 96 h, pools of embryos were thoroughly washed in clean tap water (3 times) and then stored for different purposes. Pools of 30 manually de-chorionated embryos were snap-frozen in liquid nitrogen and stored at -80 °C for biochemical assays, pools of 3 chorionated and 15 de-chorionated embryos were kept for trace metal analysis, and pools of 15 de-chorionated embryos for whole body electrolytes (Ca^{2+}, Na^{+} and Mg^{2+}).

2.4. Metal and electrolytes analysis from the sub-lethal exposure

Embryos were separated into two categories, with chorion (chorionated) and without chorion (de-chorionated). In the de-chorionated embryos, chorion and perivitelline fluid (PVF) were mechanically separated with forceps from the inner embryo. The method for trace metal determination was similar to that previously used in the laboratory (Shaw et al., 2012). De-chorionated and chorionated embryos were digested at 60 °C for 1 h in 0.5 mL of concentrated HNO_3 (68% trace element grade, Fisher Scientific, Loughborough, UK). After digestion, samples were diluted to 4 mL in ultrapure water and spiked with Indium/Iridium to a final concentration of 10 μg L^{-1} In/Ir (internal analytical standards). Triplicates were analysed for Cu (isotope ^{65}Cu) by inductively coupled plasma mass spectrometry (ICP-MS, X-Series II quadruple, Thermo Scientific, Paisley, UK) and for electrolytes (wavelengths: Ca = 397 nm, Na = 590 nm, Mg = 280 nm) by ICP-OES. Matrix matched acidified element standards were measured every 10–15 samples to check the instrument for drift and recoveries of In/Ir. Data were expressed as ng Cu, Ca, Na and Mg per embryo. The metal content of the chorion was calculated by the subtraction of Cu concentration in the de-chorionated embryos from the total amount determined for the whole (chorionated) embryos.

2.5. Biochemical analyses from the sub-lethal exposure

Biochemical analyses were performed on pools of de-chorionated embryos. Embryos were homogenised on ice (3 ×10 s) with a disposable pestle system (VWR, Lutterworth, UK) in cold isotonic buffer [300 mmol L^{-1} sucrose, 20 mmol L^{-1} 4-(2-hydroxyethyl)-1-piperazineethanesulfonic acid (HEPES), 0.1 mmol L^{-1} ethylenediaminetetraacetic acid (EDTA), pH 7.8)]. Homogenates were centrifuged (13,000 *rpm* for 2 min) and supernatants transferred to new tubes and stored at -80 °C until further analysis. Sodium pump (Na^{+}/K^{+}-ATPase) activity was measured according to McCormick, 1993 in sextuplicate reactions with 10 μL of homogenate, 50 μL of salt reaction and 150 μL of solution with/without inhibitor (ouabain, 0.5 mmol L^{-1}). Final assay concentrations were 3 U mL^{-1} of lactate dehydrogenase (LDH), 3.75 U mL^{-1} pyruvate kinase (PK), 2.1 mmol L^{-1} phosphoenolpyruvate (PEP), 0.53 mmol L^{-1} adenosine triphosphate (ATP), 0.16 mmol L^{-1} nicotinamide adenine dinucleotide (NADH), 37.25 mmol L^{-1} HEPES, 47.25 mmol L^{-1} NaCl, 2.63 mmol L^{-1} $MgCl_2$, 10.5 mmol L^{-1} KCl, at pH 7.5. Reactions were monitored by the disappearance of NADH at 340 nm every 10 s for 10 min on a VersaMax microplate reader (Molecular Device Ltd, Wokingham, UK).

Total glutathione (tGSH) determination was adapted from Baker et al. (1990) and measured in triplicate reactions, using 20 μL of supernatant and 180 μL of master mix. Final assay concentrations were 76.5 mmol L^{-1} of phosphate buffer (pH 7.5), 3.8 mmol L^{-1} of EDTA, 0.12 U mL^{-1} of glutathione reductase (GR), 0.5 mmol L^{-1} of 5′5′-dithiobis-2-nitrobenzoic acid (DTNB), 0.2 mmol L^{-1} of β-nicotinamide adenine dinucleotide phosphate tetrasodium salt (NADPH). Reactions were monitored by the increase of absorbance at 412 nm every 15 s for 10 min on the Versa max microplate reader. Superoxide dismutase (SOD) activity was measured in triplicate reactions, using 20 μL of supernatant and a SOD determination kit (product 19160, Sigma-Aldrich). The reaction was monitored by the formation of the superoxide anion at 450 nm by a single read on the VersaMax microplate reader. Na^{+}/K^{+}-ATPase and SOD activities were normalised to total protein in the supernatant using Pierce™ BCA Protein Assay Kit (product 23227, Thermo Scientific).

2.6. Data analysis

All statistical analyses were performed using SigmaPlot *v.* 12.5. *A priori*, all data were tested for normality (Shapiro–Wilk test) and homogeneity of variance (Brown-Forsythe test). Where data were not normally distributed, data were transformed (log10). Statistically significant differences between treatment groups were determined by ANOVA followed by Dunnett's test or Holm-Sidak test. Where log-transformation failed, the Kruskal–Wallis test was applied as appropriate on untransformed data. Two significance levels ($P < 0.01$ and $P < 0.05$) were employed for statistical analyses. Lethal and effect concentrations values of 10% and 50% (EC_{10}, EC_{50} and LC_{10}, LC_{50}) and corresponding 95% confidence limits were calculated using a non-linear allosteric decay function. Lowest observed effect concentration (LOEC), no effect concentration (NOEC), and maximum acceptable toxicant concentration (MATC) were also calculated. All data are presented as means ± standard deviation, unless otherwise stated.

3. Results

3.1. Characterization of copper oxide nanomaterials

Images from TEM of CuO ENMs suspensions showed primary particles with a quasi-spherical shape (Fig. 1a). The measured primary particle diameter in fresh suspensions of ultrapure water was 15.31 ± 2.76 nm (mean ± S.D., $n = 35$) and smaller than the manufacturer's information (30–50 nm). Freshly prepared particles in freshwater were similar in primary diameter (14.55 ± 2.61 nm) to the ones in ultrapure water. However, aged suspensions (24 h) in freshwater had a larger diameter (20.27 ± 4.49 nm) and this was significantly different from the initial dispersion ($F_{1,69} = 43.29$, $P < 0.001$). The particle size distributions and mean hydrodynamic diameters were measured using NTA in ultrapure water over 0.5 h and no differences were found ($F_{1,63} = 0.136$, $P = 0.715$), suggesting the fresh suspensions were sufficiently stable over short periods for dosing from the stocks. Then, the same measurements were performed in freshwater over 24 h (Fig. 1b), where some progressive particle settling was observed. At 0 h immediately after dosing, most of the agglomerates of CuO ENMs were smaller than 300 nm in freshwater (>97%, Fig. 1b) and with a total particle number concentration of 798.58 × 10^6 particles mL^{-1} and a mean hydrodynamic diameter of 157.7 ± 0.94 nm. After 24 h, a relatively stable dispersion of smaller agglomerates up to 70 nm remained, but the concentration of particle number in the 90–300 nm range decreased approximately 3-fold (Fig. 1b; $F_{2,32} = 5.84$, $P < 0.001$). The mean hydrodynamic diameter of the dispersion (196.33 ± 4.92 nm) also increased after 24 h ($F_{2,8}$ =

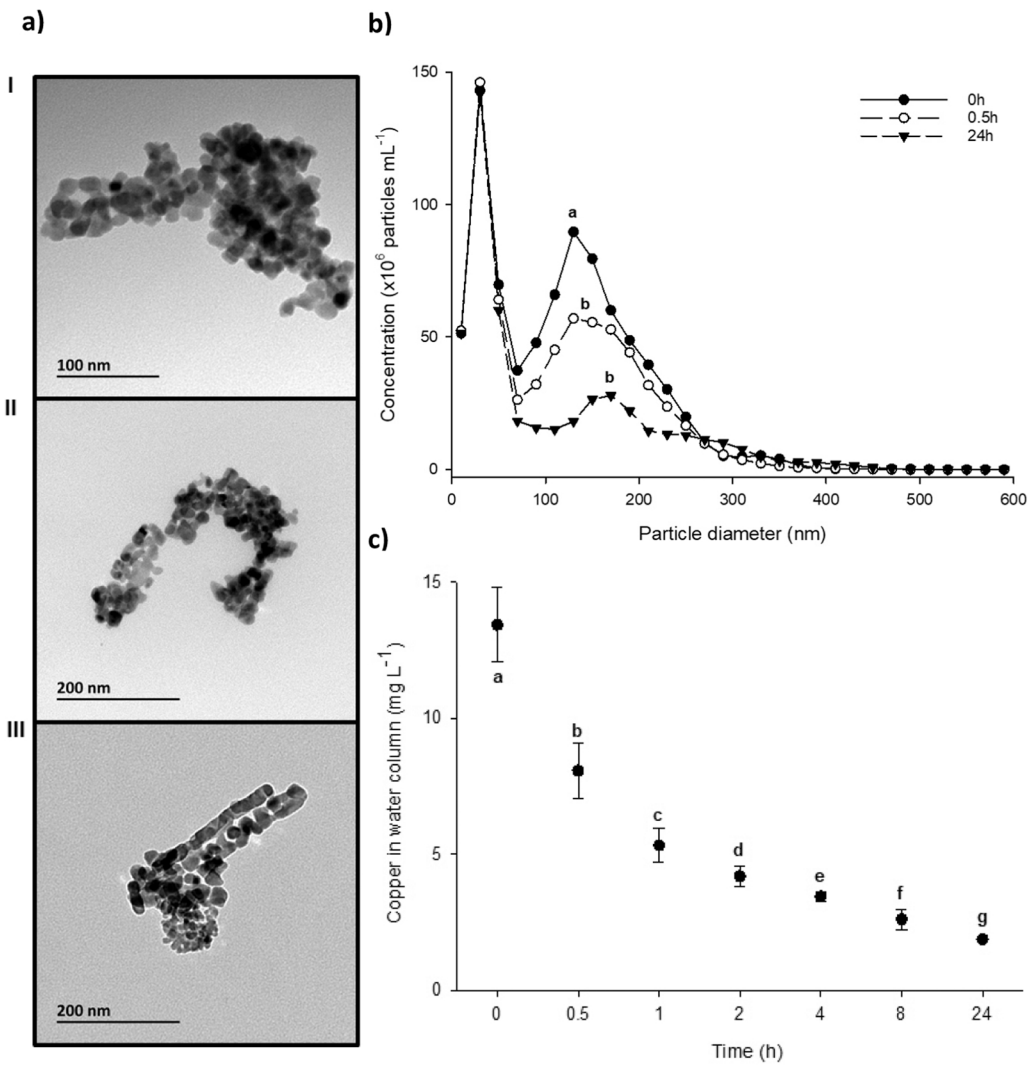

Fig. 1. Characterization of copper oxide nanomaterials (CuO ENMs) in the water column of freshwater; (a) Transmission electronic microscope (TEM) images of CuO ENMs in ultrapure water (t = 0 h, I), or freshwater water (t = 0 h, II, and 24 h, III); (b) Particle size distribution measurements of CuO ENMs obtained by Nanoparticle tracking analysis (NTA, Nanosight LM10) in freshwater. Values represent mean ± S.D. ($n = 3$ replicates of dispersion). Data points with different lower-case letters are significantly different (Holm-Sidak test, $P < 0.01$). (c) Total copper concentration in the water column of freshwater for CuO ENMs. Values are mean ± S.D. ($n = 3$). Data points with distinct lower-case letters are significantly different (Holm-Sidak test, $P < 0.05$).

57.75, P < 0.001).

The particle settling was confirmed by measuring the total Cu concentration in the water column from the CuO ENMs suspensions over 24 h (Fig. 1c). The measured total Cu concentration showed an exponential decay, decreasing from 13.43 ± 1.12 mg L^{-1} to 1.87 ± 0.09 mg L^{-1} after 24 h (Fig. 1c; $F_{2,29} = 52.53$, $P < 0.001$). However, the settling in freshwater was instantaneous, and even at 0 h (within a few minutes of mixing) only 54% of the nominal exposure concentration was retained in the water column itself.

A dialysis experiment was also conducted to explore the dissolution of dissolved Cu from the particles (Fig. 2). The $CuSO_4$ showed a hyperbolic rise to equilibrium in the beaker as expected, and the 29.5 mg of Cu as $CuSO_4$ added, reaching a plateau within two h and a steady-state concentration of 27.58 ± 1.85 mg Cu L^{-1} – equivalent to 434.02 ± 29.11 μmoles L^{-1} – for $CuSO_4$ treatment after 24 h (Fig. 2a), which represents a 28.0% of the Cu remaining as a diffused phase in the water column. The release of dissolved Cu from CuO ENMs was even lower with only 107.15 ± 8.17 μg L^{-1} of Cu from CuO ENMs in the beaker by 24 h (Fig. 2b). This represents < 0.01% dissolution of the Cu metal in freshwater from the particles in 24 h. A maximum dissolution rate of 57 μg h^{-1} was attained in the first 30 min.

3.2. Lethal effects

The lethal concentration range finding test identified both the 96 h-LC_{50} (mean ± 95% CI) for $CuSO_4$ (303.09 ± 14.44 μg Cu L^{-1}) and CuO ENMs (53.11 ± 9.86 mg L^{-1}), where the ENMs were orders of magnitude less toxic than the metal salt. Additional, sub-lethal endpoints were measured in the lethal concentration test regarding hatching success, "perivitelline fluid morphology" and the presence of ENMs sticking to the surface of the chorion (Fig. 3). The $CuSO_4$-exposed embryos exhibited a negative correlation between hatching success and "perivitelline fluid morphology" (Pearson coefficient = -0.773, $P < 0.0001$) (Fig. 3a and c); that is, embryos that did not have a clear and healthy perivitelline fluid also tended not to hatch (Fig. 3e). The embryos exposed to CuO ENMs also showed a strong negative correlation between hatching success and the surface coating of chorion with particulates (Pearson coefficient = −0.804, $P < 0.0001$) (i.e., embryos with a chorion visually surrounded with ENMs tended not to hatch, Fig. 3f). At CuO ENM concentrations ≥ 50 mg L^{-1} there was a 100% incidence of embryos with particles coating the surface, and negligible hatching success (Fig. 3b and d). The effective concentration (EC) values were calculated for these endpoints: the 96 h-EC_{50} of the proportions of embryos showing increased "perivitelline fluid morphology" was 220.58 ± 5.23 μg Cu L^{-1} ($CuSO_4$) and the 96 h-EC_{50} for the proportion of embryos with a surface coated chorion was 6.05 ± 1 mg L^{-1} (CuO ENMs). Considering hatching inhibition, for both Cu forms the 96 h-EC_{50} was 68.5 ± 18.6 μg Cu L^{-1} ($CuSO_4$) and 0.92 ± 1.46 mg L^{-1} (CuO ENMs). The 96 h-LC_{10} values for $CuSO_4$ (197.7 ± 120.03 μg Cu L^{-1}) and CuO ENMs (20.76 ± 33.51 mg L^{-1}) were also identified in the ranging lethal

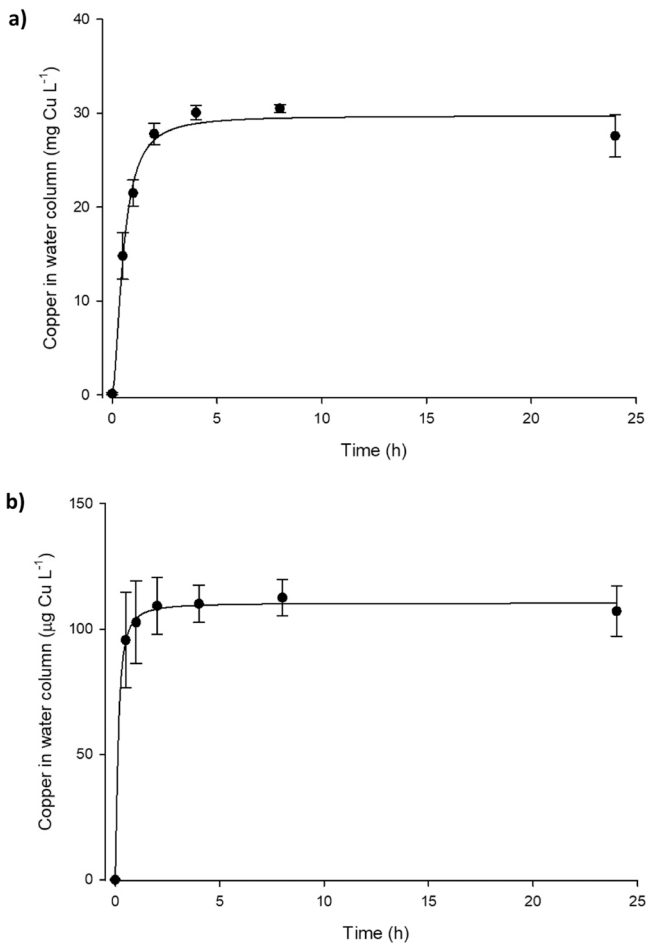

Fig. 2. Total dissolved copper concentration measured in the water column during equilibrium dialysis over 24 h; (a) $CuSO_4$ and, (b) CuO ENMs. Note the difference in scales on the y-axis. Values are mean ± S.D. ($n = 3$ independent replicates). Curves were fitted using a rectangular hyperbola function in SigmaPlot $CuSO_4$ [r^2= 0.974, y = ((29.71 *x)^1.75)/((0.522^1.75)+ (x^1.75))] and CuO ENMs [r^2= 0.936, y = ((110.35 *x)^1.44)/((0.139^1.44)+ (x^1.44))].

concentration finding test and these values were then used for the main sub-lethal exposure experiments.

3.3. Sub-lethal exposure and metal distribution in zebrafish embryos

The sub-lethal exposure to either $CuSO_4$ or CuO ENMs was confirmed by measuring the total Cu concentrations in the media (Fig. 4) and in the embryos (Fig. 5). For the exposure media, the total Cu concentration from $CuSO_4$ was reasonably close to nominal concentration ($t = -5.77$, $H = 10$, $P < 0.001$). The CuO ENMs suspensions (Fig. 4b), as expected, showed some particle settling with the measured Cu concentration in the water column decreasing 7-fold to 1.77 mg L^{-1} by the end of the experiment ($t = 44.11$, $H = 10$, $P < 0.001$). Nonetheless, the embryos were exposed to mg L^{-1} dose of CuO ENMs. The total Cu in the embryos reflected the exposures (Fig. 5). For $CuSO_4$, the chorion was not a barrier to the dissolved metal and Cu was readily measured in both chorionated and de-chorionated embryos, where 42.2% of copper was associated to the inner embryo and perivitelline space and 57.8% of copper was associated to the chorion (Fig. 5a, 2-fold difference). Regarding the exposure to CuO ENMs, the whole-body Cu mass in chorionated embryos was higher than in the de-chorionated ones (17-fold difference; $F_{2,33} = 83.37$, $P < 0.001$), indicating that most of the total copper measured was retained on the chorion (94.2%), not in, the embryo. Nonetheless, a few hundred ng of Cu were measured in the de-chorionated embryos (5.8% of copper), confirming that the embryos were effectively exposed.

3.4. Osmoregulation and oxidative stress during sub-lethal exposures

Copper sulphate ($CuSO_4$) is known to interfere with ion homeostasis and the de-chorionated embryos showed evidence of depletion of Ca^{2+} ($F_{2,13} = 32.22$, $P < 0.001$) and Na^+ ($F_{2,13} = 8.47$, $P = 0.006$), but not Mg^{2+} (Table 1). This occurred with inhibition of the total Na^+/K^+-ATPase (Fig. 6a; $F_{2,12} = 4.66$, $P = 0.037$). A similar depletion of Ca^{2+} and Na^+ was observed in the CuO ENMs exposure (Table 1), but unlike $CuSO_4$, CuO ENMs did not inhibit the Na^+/K^+-ATPase (Fig. 6a). Embryos also showed evidence of oxidative stress, with depletion of tGSH in embryos exposed to either $CuSO_4$ or CuO ENMs (Fig. 6b; $F_{2,16} = 38.26$, $P < 0.001$). However, this trend was not accompanied by an increase SOD activity which remained unchanged in all treatments (Fig. 6c; $F_{2,16} = 2.87$, $P = 0.09$).

4. Discussion

This study shows that $CuSO_4$ is much more toxic to zebrafish embryos than CuO ENMs, and for the metal salt, the increase in the proportion of embryos with bubbles and foam-looking perivitelline fluid was associated with poor hatching success. In the case of the acute CuO ENM exposures, the chorion became smothered in particulate material, and this was associated with failure to hatch during the acute toxicity study. In the sub-lethal exposure, the chorion, as expected, was not a barrier to the accumulation of Cu from $CuSO_4$ inside the embryo. In contrast, for the CuO ENM exposure, a large proportion of the total Cu was associated with the chorion, although some total Cu (form unknown) was internalised resulting in exposure of the embryos. In terms of the mechanisms of sub-lethal toxicity, both $CuSO_4$ or CuO ENMs caused electrolyte depletion of the embryos, and $CuSO_4$ caused some inhibition of the Na^+ pump activity. Both forms of Cu exposure caused some deletion of total GSH in the embryos, but this oxidative stress was not sufficient to induce superoxide dismutase activity.

4.1. Acute toxicity of $CuSO_4$ compared to CuO ENMs during lethal exposures

In the present study, the 48 h LC_{50} for the zebrafish early life stage with $CuSO_4$ was around 0.3 mg L^{-1} compared to 52 mg L^{-1} for CuO ENMs (Table S1); with the nanomaterial being at least two orders of magnitude less toxic than the metal salt. The lethal concentration values report here for $CuSO_4$ (Table S1) are broadly in keeping with previous reports on Cu salts. For example, Griffitt et al. (2008) reported a 48 h LC_{50} for $CuCl_2$ of 1.78 mg L^{-1} in moderately hard water. Freiry et al. (2014) reported a 48 h LC_{50} for $CuSO_4$ of around 0.3 mg L^{-1} in 10-day old zebrafish. Studies on CuO ENMs with zebrafish early life stages have also shown that the nanomaterial form is toxic at tens of mg L^{-1} or more, and therefore much less hazardous than the metal salt. For example, the 48 hpf LC_{50} value for zebrafish was about 64 mg L^{-1} for CuO ENMs with a primary particle diameter of about 60 nm (Ganesan et al., 2016). Similarly, Vicario-Pares et al. (2014) reported LC_{50} estimates of > 10 mg L^{-1} for early life stages of zebrafish exposed to CuO ENMs. Contrary to these reports on CuO ENMs, Griffitt et al. (2008) reported a 48 h LC_{50} of 0.71 mg L^{-1} for a Cu metal ENM, which was 2.5 times more toxic than the metal salt control. So, clearly the composition of the ENM is important and the metal oxide is a less hazardous nano form. Interestingly, Thit et al. (2017) found that zebrafish embryos exposed to equimolar concentrations of Cu as $CuCl_2$ or very small CuO ENMs (6 nm primary size) showed similar toxicities over 24 h; but the hatch larvae showed differential sensitivity with the metal salt being much more toxic at concentrations of 50 µMol L^{-1} or more. Shaw et al. (2016) reported that the hatched larvae are more sensitive to a range of ENMs that the embryos in the fish early life stage test. So, qualifying when the embryos hatch in a study will be important to the

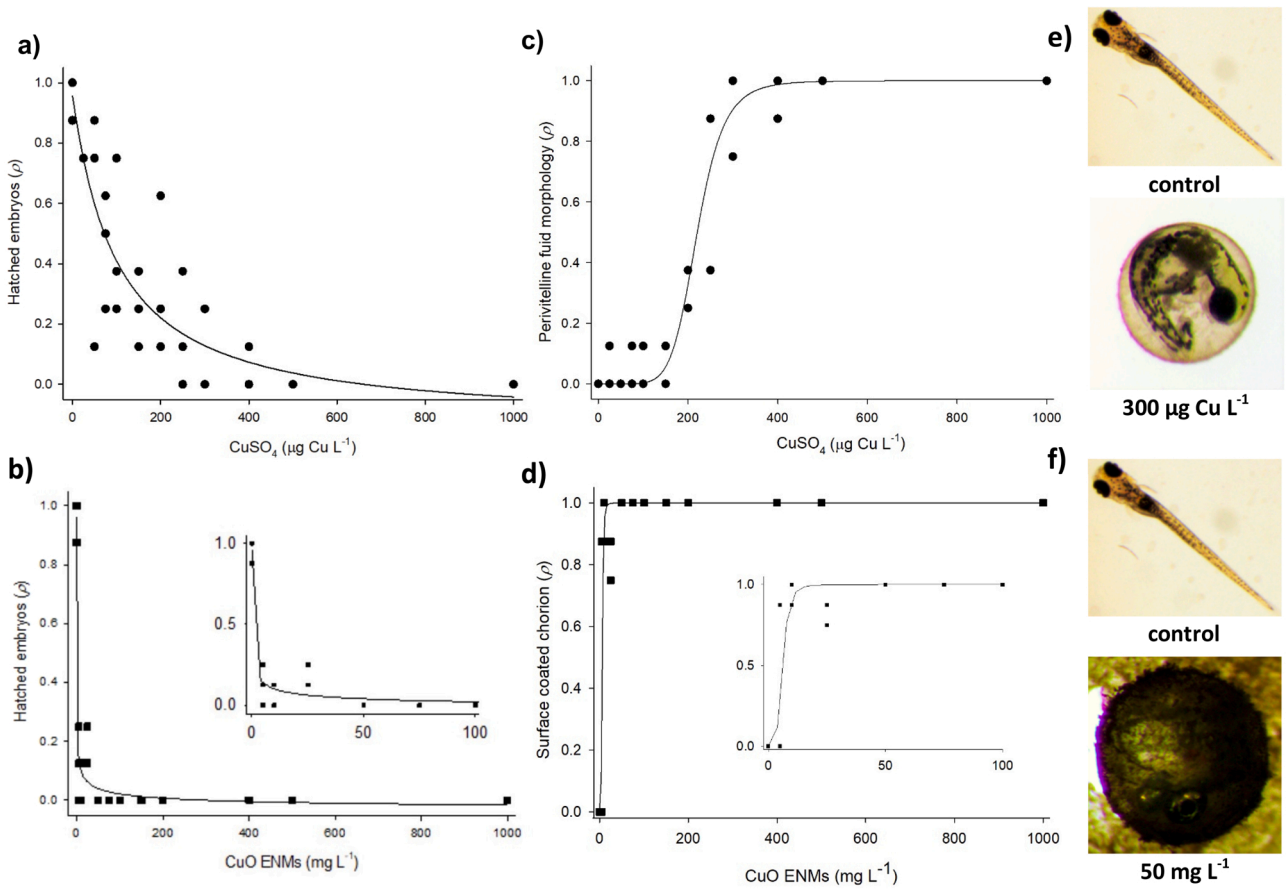

Fig. 3. Effects of $CuSO_4$ (a, c and e) and CuO ENMs (b, d and f) on zebrafish embryos resulting from lethal exposures over 96 hpf. Curves in panels (a) to (d) are embryos ($n = 24$) represented as independent replicates. Hatching success refers the proportion (ρ) of embryos that successfully hatched in $CuSO_4$ (filled circles in panel **a**) and CuO ENMs (filled squares in panel b). Curves were fitted using Sigmaplot and were based on the sigmoidal functions of $CuSO_4$ [$r^2 = 0.774$, $y =$ ((−0.13)+ ((0.96 +0.13)* (98.86^1.05)))/((98.86^1.05)+ (x^1.05))] and CuO ENMs [$r^2 = 0958$, $y =$ ((−0.045)+ ((0.96 +0.045)* (0.095^0.382)))/((0.095^0.382)+ (x^0.382))] data, respectively. "Perivitelline fluid morphology" indicates the proportion (ρ) of embryos with a perivitelline fluid with bubbles and a foam-looking, unlike the control in the $CuSO_4$ treatment (filled circles in panel c). "Surface coated chorion" indicates the proportion (ρ) of embryos with the chorion visually covered with adsorbed particulate materials (the ENMs) (filled squares in panel d). Curves were based on sigmoidal functions of $CuSO_4$ [$r^2 = 0.956$, $y = (x$^7.32)/((220.58^7.32)+ (x^7.32))] and CuO ENMs [$r^2 = 0.853$, $y = (x$^4.61)/((6.05^4.61)+ (x^4.61))], respectively. Images in panels (e) and (f) show the typical morphology, from the $CuSO_4$ (300 µg Cu L^{-1}) and CuO ENMs (50 mg L^{-1}) treatments, on 96hpf old zebrafish embryos or larvae against the respective controls.

interpretation of the cumulative toxicity over time, and to understanding the Cu exposure of the fish inside the embryo (see below). Notably, in the present study, regardless of the form of Cu exposure, the LC_{50} estimates at 48, 72 and 96 hpf within each substance were very similar (Fig. S1; Table S1), indicating that most of the toxicity occurred in the first 48 hpf of the exposure (i.e., before hatching).

4.2. Sub-lethal exposure and total Cu accumulation

Exposure to Cu was confirmed in the sub-lethal experiment by measuring the total Cu concentrations in the freshwater (Fig. 4) and in the zebrafish (Fig. 5). In $CuSO_4$, the initial total Cu concentration measured in the test vessels was around 120 µg L^{-1} and 39% lower than the nominal concentration of 190 µg Cu L^{-1}. This to be expected as microgram amounts of Cu can be instantly adsorbed to the walls of the test containers, the surface of the organism and chelated by mucous secretions. Indeed, an OECD validation study of the zebrafish test also reported measured concentrations of Cu as $CuSO_4$ in the media that were some 37% lower than the nominal exposure concentration (Busquet et al., 2014). Nonetheless, despite these initial losses, the concentration of Cu was stable in the exposure solution over 24 h (the duration to the next water change) and the presence of Cu in the water column was confirmed (Fig. 4a). The calculated Cu speciation (Visual MINTEQ version 3.1 https://vminteq.lwr.kth.se/) was: Cu^{2+}, 60.80%; $CuOH^{+}$, 33.93%; $Cu(OH)_2$ (aq), 1.35%; $Cu_2(OH)_2^{2+}$, 2.55%; $Cu_3(OH)_4^{2+}$, 0.11%; $CuCl^{+}$, 0.30%; $CuSO_4$ (aq), 0.94%. Thus, as expected about two thirds were as dissolved Cu^{2+} and the remained mostly as copper hydroxide complexes. The calculated free Cu^{2+} ion activity was 1.35 µmol L^{-1} (or 86 ug L^{-1}) and consistent with the exposure. For the CuO ENMs, the initial Cu concentration in the exposure suspension was 28% lower than the nominal concentration (20 mg L^{-1}) and then dropped by 86% over 24 h, so that only a few mg L^{-1} of total Cu remained in the water column (Fig. 4b). This was attributed to particle settling from the water column due to aggregation (Fig. 1). Similar observations were made by Boyle et al. (2020), where particle settling of the CuO ENMs in the media removed most of the total Cu from the water column. While particle settling due to the ionic strength and composition of the media is unavoidable in semi-static exposure methods [without adding dispersing agents, mixing, etc. (Handy et al., 2012)], there was, nonetheless, a few mg L^{-1} of Cu as CuO ENMs remaining at the end of every 24 h (Fig. 4b), and renewal of the test media helped to ensure the supply of CuO ENM was in excess throughout the exposure. Crucially, any CuO ENM settling from the water column would inevitably come into direct contact with the embryos in the bottom of the test vessels. Additionally, equilibrium dialysis data showed that the total Cu concentration outside the bag were as expected for $CuSO_4$, with 29.5 mg of total Cu added to the bag diffusing to the external compartment. For CuO EMNs, with 7.5 mg of material added to the dialysis bag, but only µg L^{-1} concentrations of Cu

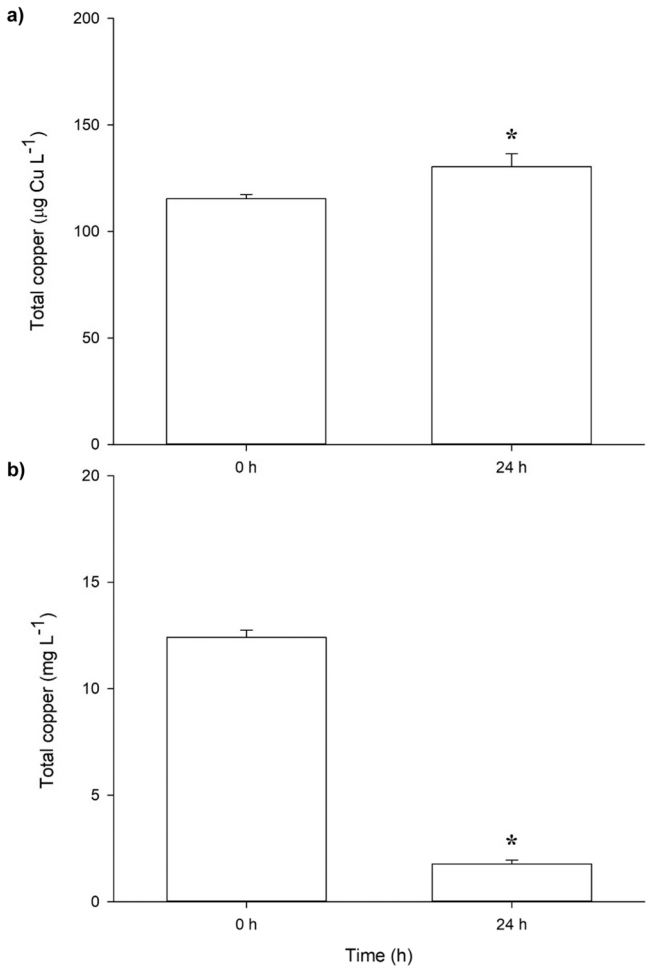

Fig. 4. Total copper (Cu) concentrations in the freshwater during sub-lethal exposure of zebrafish to nominal concentrations of, (a) 190 µg Cu L^{-1} presented as $CuSO_4$, or (b) as 20 mg L^{-1} of CuO ENMs. Data for the water from the controls are not shown (values all below the detection limit, < 1.82 µg L^{-1}). Values are mean ± S.D. ($n = 6$). Bars with asterisks are significantly different (*t-test, $P < 0.001$).*

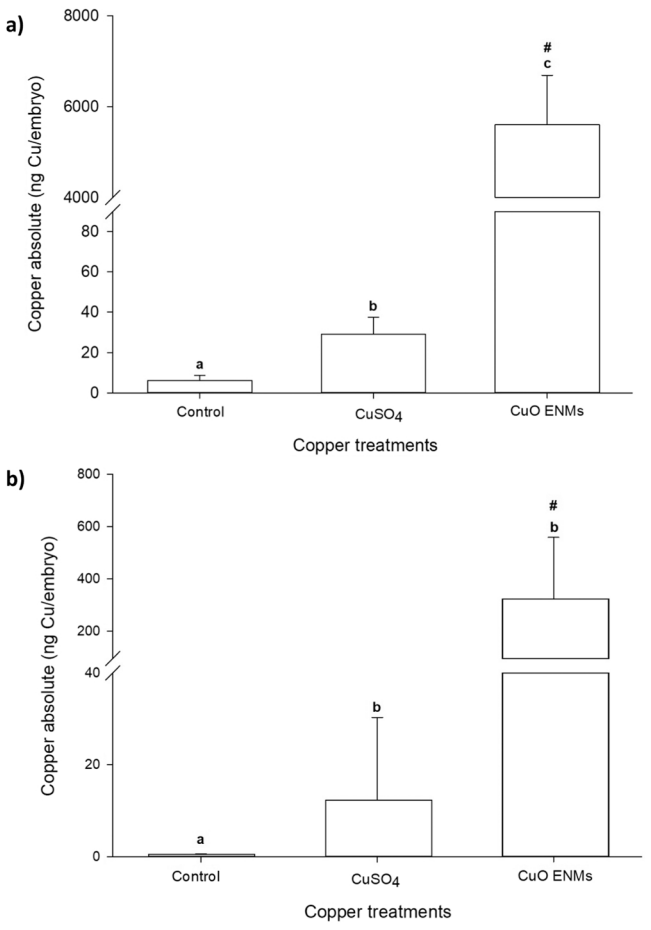

Fig. 5. Total absolute mass of copper (ng per embryo) in, (a) chorionated, and (b) de-chorionated zebrafish embryos exposed to the respective nominal 96 h-LC_{10} ($CuSO_4$ = 190 µg Cu L^{-1} and CuO ENMs = 20 mg L^{-1}). Values are means ± S.D. ($n = 3 – 9$ independent samples of embryos). Bars with different lower-case letters and cardinal symbol (#) are significantly different within and/or between chorionated and de-chorionated embryos, respectively (one-way ANOVA, Holm-Sidak test, $P < 0.01$).

were released by dissolution, suggesting the CuO ENMs are very sparingly soluble and remained in the particulate form during the experiments.

The measured total Cu concentrations in the embryos also confirmed the exposure (Fig. 5). The intact (chorionated) embryos from both forms of Cu exposure showed significantly higher Cu concentrations than the unexposed controls. The Cu concentration on/in the intact embryos was much higher from the CuO ENM exposure than the $CuSO_4$ exposure, in keeping with the different exposure concentrations (LC_{10} values) of the substances (Fig. 5a). Notably, total Cu (form unknown) was taken up into the embryos in both the $CuSO_4$ and CuO ENM exposures (Fig. 5b). For $CuSO_4$ exposures, about 42% of the total Cu associated with the embryos was internally located as measured in de-chorionated animals (i.e., around 58% of the total Cu on/associated with the chorion). Other studies on dissolved metals show around two thirds or slightly more of metal is on/associated with the chorion, for example, cadmium [61% in zebrafish (Burnison et al., 2006)], and silver [65–85% in rainbow trout (Guadagnolo et al., 2001)].

In contrast to $CuSO_4$, the de-chorionated embryos from the CuO EMN exposure had only some 350 ng/embryo compared to around 6000 ng/embryo on/in the chorionated counterparts (Fig. 5); indicating that most (~94%) of the Cu from the CuO ENM exposure was located on the exterior of the animals and that the chorion was a reasonably effective barrier to prevent the internalisation of the nanomaterial, at least in the short term. That is, the CuO ENMs were bioaccessible to the exterior of the chorion, but not bioavailable to the animal inside the embryo. The pore canal diameter on the zebrafish chorion is about 0.7–0.9 µm (Chen et al., 2020), indicating that it would probably not stop the diffusion of any monodispersed primary particles (~60 nm), but with aggregates of 0.15–0.3 µm in freshwater (Fig. 1b), only a few aggregates at the size would be needed to block the exterior surface of the pores. Notably, particulate material coated the surface of the chorion in the CuO ENM exposures (Fig. 3), in keeping with this suggestion.

Table 1
Total electrolyte concentrations in de-chorionated zebrafish embryos following 96 h exposure to a sub-lethal (LC_{10}) concentration of either $CuSO_4$ or CuO ENMs.

Electrolyte (ng per embryo)	Control ($n = 3$)	$CuSO_4$ ($n = 7$)	CuO ENMs ($n = 4$)
Calcium	210.77 ± 22.72^a	100.67 ± 21.79^b	98.65 ± 4.3^b
Magnesium	133.52 ± 21.08^a	102.26 ± 23.61^a	101.08 ± 27.38^a
Sodium	256.02 ± 44.81^a	149.51 ± 44.42^b	122.66 ± 31.07^b

Values are means ± standard deviation (n = replicate samples of embryos). Different lower-case letters are significantly different within rows (one-way ANOVA; Holm-Sidak test, $P < 0.05$).

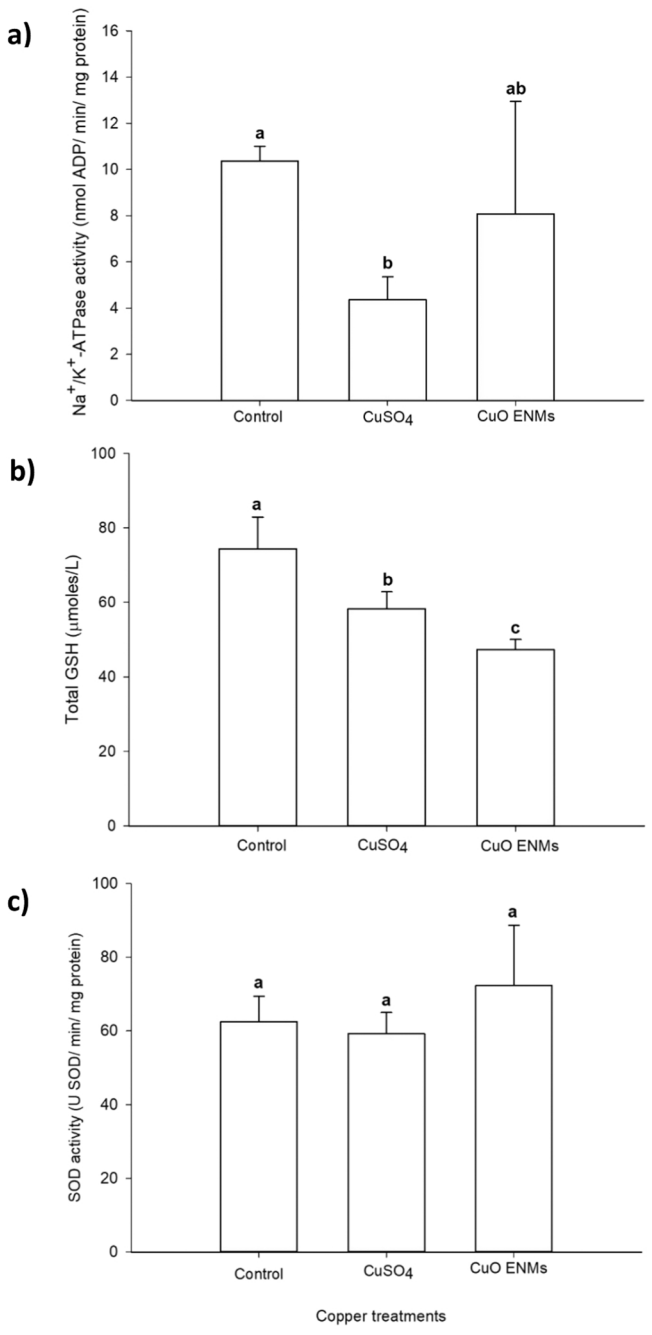

Fig. 6. Biochemical responses of de-chorionated zebrafish embryos exposed to the respective nominal 96 h LC_{10} of $CuSO_4$ (190 µg Cu L^{-1}) or CuO ENMs (20 mg L^{-1}); (a) sodium pump (Na^+/K^+-ATPase) activity, (b) total glutathione (Total GSH) levels, and (c) superoxide dismutase (SOD) activity. Values are mean ± S.D. (*n = 3 – 6 independent samples of embryos*). Bars with different lower-case letters are significantly different (one-way ANOVA, Holm-Sidak test, $P < 0.05$).

4.3. Hatching success in the lethal exposure

The hatching success of fish embryos typically depends on the anatomical maturity of the fish and their ability to endure the energetic demands of hatching, as well as the integrity of the perivitelline fluid and chorion. Unfortunately, the bubbles and foam-looking nature of the perivitelline fluid ($CuSO_4$ exposures), or the particulate coating on the embryos (CuO ENM exposures), prevented any useful morphometric measurements on the fish inside the embryos. However, it was clear that failure to hatch in the $CuSO_4$ treated was partly correlated with the proportion of embryos with a dense-looking perivitelline fluid (Fig. 3a). Perivitelline fluid consists of electrolytes trapped in a polyanionic matrix of mucoproteins (Eddy and Handy, 2012). Mucoproteins have an affinity for Cu ions (Miller and Mackay, 1982), and it is, therefore, no surprise that some total Cu from $CuSO_4$ appeared in the embryos (Fig. 5); but occurred with some denaturing of the perivitelline fluid (observed as bubbles and foam-looking embryos, Fig. 3). The latter effect on the perivitelline fluid could arise from some oxidative stress during the $CuSO_4$ exposure (Fig. 6). It was not the purpose of the current study to determine the mechanism of failure to hatch with $CuSO_4$, but for example, impaired oxygen diffusion to the fish inside the embryo (Pelster and Bagatto, 2010), and/or increased viscosity of the perivitelline fluid might impede the physiological ability (i.e., exercise performance) of the fish to breach through the chorion. Another factor for hatching is the action of the proteolytic enzyme ZHE_1 that is released in the perivitelline space to weaken the chorion, but it can be inhibited by Cu^{2+} (Muller et al., 2015). Regardless of the mechanism, in the present study, $CuSO_4$ inhibited hatching ($\mathbf{EC_{50}}$ = 68.5 µg Cu L^{-1}) at a similar dose to that reported previously with zebrafish embryos [$\mathbf{EC_{50}}$ = 60 µg Cu L^{-1} Bai et al. (2010)].

Embryos exposed to CuO ENMs exhibited a particulate surface coating over the chorion and this was correlated with the failure to hatch (Fig. 3d and Fig. S3). In addition to the mechanisms above for $CuSO_4$ and any local release of Cu ions from CuO ENMs, the smothering of the chorion could impede gas exchange and/or the elimination of nitrogen waste, increasing toxicity within the perivitelline fluid. Previous studies showed hatching inhibition by mg L^{-1} amounts of CuO ENMs (Ganesan et al., 2016; Kumari et al., 2017; Muller et al., 2015) or Cu ENMs (Bai et al., 2010); consistent with the present study and at much higher concentrations than $CuSO_4$. In zebrafish embryos exposed to ZnO ENMs, loss of the protease activity needed to weaken the chorion also explained inability to hatch, but notably, if the embryos were manually de-chorionated, the fish survived (Ong et al., 2014).

4.4. Osmoregulation and oxidative stress in sub-lethal exposure

The electrolyte concentrations in de-chorionated embryos showed some depletion of both total Ca^{2+} and Na^+ from animals during the Cu exposures compared to unexposed controls; but with no difference between the metal salt and CuO ENMs in this effect (Table 1). This is most likely explained by passive electrolyte losses from the altered (dense-looking, presumed denatured) perivitelline fluid during the exposures, and some ion exchange with any external Cu ions. For the latter, Cu^{2+} is well-known for its competition with Na^+ and perhaps Ca^{2+} (Handy et al., 2002). Metals have been previously reported to cause Na^+ depletion in fish embryos by such mechanisms [e.g., acid (McWilliams and Shephard, 1991)]. However, the Mg^{2+} concentration was not depleted (Table 1), likely because the Mg^{2+} ion activity in freshwater fish embryos is normally close to the equilibrium potential with the surrounding water (see, Van der Velden et al., 1991), therefore, not so easily lost by diffusion. Previous studies, Alsop and Wood (2011) also reported stable total Mg^{2+} concentrations in fish exposed to dissolved Cu.

The perivitelline fluid is designed to buffer the fish from changes in the external environment, and so any electrolyte depletion might add a subsequent osmotic stress to the animal. Some direct interference with ionic regulation in the fish is probable in the case of $CuSO_4$, where inhibition of the Na^+/K^+-ATPase was observed (Fig. 6). Inhibition of the sodium pump during dissolved Cu exposure is well-known in fish (Handy et al., 2002), with consequent Na^+ depletion. Calcium losses might then arise indirectly from the subsequent disruption of secondary Na^+/Ca^{2+} exchange in the gills which relies ultimately on the Na^+ pump for energy (Bury and Handy, 2010), or simply by damage to the tissue (oxidative stress via glutathione depletion, Fig. 6). Significant losses of Ca^{2+} and Na^+ (to a larger extent) were also reported in zebrafish larvae exposed to 100 µg Cu L^{-1} (Alsop and Wood, 2011). Notably, the

exposure to CuO ENMs causes slightly more tGSH depletion than that of $CuSO_4$ exposure (Fig. 6b), and although the Na^+ pump activity was not statistically decreased for the CuO ENM treatment, there was some considerable variation in specific activity (Fig. 6a), suggesting that sodium homeostasis was approaching a threshold for inhibition. Inhibition of Na^+/K^+-ATPase activity has been reported in fish exposed to Cu ENMs and CuO ENMs (Ganesan et al., 2016; Shaw et al., 2012; Wang et al., 2014).

The Cu-dependent inhibition of the Na^+/K^+-ATPase can have an ionic basis where Cu^{2+} binds to thiols on the tertiary structure of the enzyme and/or interferes with the Mg^{2+} binding site (Handy et al., 2002; Li et al., 1996). However, there is an indirect mechanism where the general oxidative stress in the tissue from Cu exposure can inhibit the Na^+ pump, and this is possible given some depletion of tGSH (Fig. 6b). However, the apparent oxidative stress was only moderate because the tGSH loss was partial (Fig. 6b) and there was no induction of SOD activity in embryos exposed to $CuSO_4$ or CuO ENMs (Fig. 6c). Notably, SOD activity has been reported to increase (Gupta et al., 2016) or decrease (Ganesan et al., 2016; Sun et al., 2016; Wang et al., 2015) in fish exposed to Cu ENMs or CuO ENMs; and the activation of the Cu-dependent SOD isoforms will depend on the internal free Cu ion concentrations in the organism, as well as the overall level of oxidative stress in the different internal organs used to make the homogenates for the enzymology in each study.

4.5. Conclusions

In conclusion, this study shows that $CuSO_4$ is much more toxic than CuO ENMs to zebrafish embryos in terms of both acute mortality and failure to hatch. From an ecological perspective, the existing environmental risk assessment for the metal salt should be protective of fish populations for the nano form. However, environmental fate should also be considered, and it is likely the settling of CuO ENMs from the water column would put any fish embryos in the river sediment at risk of exposure. Notably, there were some subtle differences in the exposure and mechanisms, with the CuO ENMs mostly on/associated with the chorion barrier. In the sub-lethal studies, both substances caused electrolyte depletion, but despite internalising some Cu (form unknown), the CuO ENM exposure did not inhibit the Na^+ pump, unlike the metal salt. However, some secondary oxidative damage to the osmoregulatory machinery from the CuO ENMs could not be exclude. Finally, from an animal welfare perspective it is desirable to find alternatives to mortality as an endpoint, and here the EC_{50} values for the inhibition of hatching were more sensitive than mortality. Notably, the EC_{50} values for the proportions of embryos with foam-looking perivitelline fluid ($CuSO_4$) or with a particulate coated chorion (CuO ENMs) were also more sensitive than mortality; suggesting morphology as an alternative to mortality and perhaps an opportunity to shorten the fish early life stage test.

CRediT authorship contribution statement

Pereira conducted the experiments with support at the bench from DB, and analysed the data. All authors were involved in preparing the manuscript for submission, and the revision with input from RDH and AN. Both RDH and AN enabled funding of the research.

Declaration of Competing Interest

The authors declare that they have no known competing financial interests or personal relationships that could have appeared to influence the work reported in this paper.

Data Availability

See corresponding author with data enquiries.

Acknowledgements

SP was supported by a research scholarship from the Portuguese Foundation for Science & Technology (SRH/BD/97877/2013). DB and RDH were supported by the Sustainable Nanotechnologies Project (SUN) grant, contract number 604305 funded under the EU FP7 research programme. The research was also partly supported by the EU FP7 NANOSOLUTIONS Project, grant agreement no. 309329. RDH was the PI at the University of Plymouth. The authors thank Andrew Atfield for technical support in biology, Benjamin Eynon for technical support in the aquatics facility, and Drs Andrew Fisher and Robert Clough for support on trace metal analysis.

Appendix A. Supporting information

Supplementary data associated with this article can be found in the online version at doi:10.1016/j.ecoenv.2023.114613.

References

Al-Bairuty, G.A., et al., 2016. Sublethal effects of copper sulphate compared to copper nanoparticles in rainbow trout (*Oncorhynchus mykiss*) at low pH: physiology and metal accumulation. Aquat. Toxicol. 174, 188–198. https://doi.org/10.1016/j.aquatox.2016.02.006.

Alsop, D., Wood, C.M., 2011. Metal uptake and acute toxicity in zebrafish: common mechanisms across multiple metals. Aquat. Toxicol. 105, 385–393. https://doi.org/10.1016/j.aquatox.2011.07.010.

Amde, M., et al., 2017. Transformation and bioavailability of metal oxide nanoparticles in aquatic and terrestrial environments. A review. Environ. Pollut. 230, 250–267. https://doi.org/10.1016/j.envpol.2017.06.064.

Bai, W., et al., 2010. Effects of copper nanoparticles on the development of zebrafish embryos. J. Nanosci. Nanotechnol. 10, 8670–8676. https://doi.org/10.1166/jnn.2010.2686.

Baker, M.A., et al., 1990. Microtiter plate assay for the measurement of glutathione and glutathione disulfide in large numbers of biological samples. Anal. Biochem. 190, 360–365. https://doi.org/10.1016/0003-2697(90)90208-q.

Besinis, A., et al., 2014. The antibacterial effects of silver, titanium dioxide and silica dioxide nanoparticles compared to the dental disinfectant chlorhexidine on *Streptococcus mutans* using a suite of bioassays. Nanotoxicology 8, 1–16. https://doi.org/10.3109/17435390.2012.742935.

Boyle, D., et al., 2020. Toxicities of copper oxide nanomaterial and copper sulphate in early life stage zebrafish: effects of pH and intermittent pulse exposure. Ecotoxicol. Environ. Saf. 190, 109985 https://doi.org/10.1016/j.ecoenv.2019.109985.

Burnison, B.K., et al., 2006. Cadmium accumulation in zebrafish (*Danio rerio*) eggs is modulated by dissolved organic matter (DOM). Aquat. Toxicol. 79, 185–191. https://doi.org/10.1016/j.aquatox.2006.06.010.

Bury, N.C., Handy, R.D., 2010. Copper and iron uptake in teleost fish. In: Bury, N.C., Handy, R.D. (Eds.), Surface Chemistry, Bioavailability and Metal Homeostasis in Aquatic Organisms: An integrated approach. Society for Experimental Biology Press, London, pp. 107–127.

Busquet, F., et al., 2014. OECD validation study to assess intra- and inter-laboratory reproducibility of the zebrafish embryo toxicity test for acute aquatic toxicity testing. Regul. Toxicol. Pharmacol. 69, 496–511. https://doi.org/10.1016/j.yrtph.2014.05.018.

Chen, Z.Y., et al., 2020. The effect of the chorion on size-dependent acute toxicity and underlying mechanisms of amine-modified silver nanoparticles in zebrafish embryos. Int. J. Mol. Sci. 21, 2864. https://doi.org/10.3390/ijms21082864.

Eddy, F.B., Handy, R.D., 2012. Ecological and Environmental Physiology of Fishes, first ed. Oxford University Press, Oxford. https://doi.org/10.1093/acprof:oso/9780199540945.001.0001.

Eyckmans, M., et al., 2011. Exposure to waterborne copper reveals differences in oxidative stress response in three freshwater fish species. Aquat. Toxicol. 103, 112–120. https://doi.org/10.1016/j.aquatox.2011.02.010.

Freiry, R., et al., 2014. Sensitivity of *Danio rerio* (Teleostei, Cyprinidae) during two stages of development based on acute toxicity tests. Bull. Environ. Contam. Toxicol. 93, 442–445. https://doi.org/10.1007/s00128-014-1367-6.

Ganesan, S., et al., 2016. Acute and sub-lethal exposure to copper oxide nanoparticles causes oxidative stress and teratogenicity in zebrafish embryos. J. Appl. Toxicol. 36, 554–567. https://doi.org/10.1002/jat.3224.

Griffitt, R.J., et al., 2007. Exposure to copper nanoparticles causes gill injury and acute lethality in zebrafish (*Danio rerio*). Environ. Sci. Technol. 41, 8178–8186. https://doi.org/10.1021/es071235e.

Griffitt, R.J., et al., 2008. Effects of particle composition and species on toxicity of metallic nanomaterials in aquatic organisms. Environ. Toxicol. Chem. 27, 1972–1978. https://doi.org/10.1897/08-002.1.

Grosell, M., et al., 2002. Sodium turnover rate determines sensitivity to acute copper and silver exposure in freshwater animals. Comp. Biochem. Physiol. C: Toxicol. Pharmacol. 133, 287–303. https://doi.org/10.1016/S1532-0456(02)00085-6.

Grosell, M., 2011. Copper. In: Wood, C.M., et al. (Eds.), Homeostasis and Toxicology of Essential Metals. Academic Press, San Diego, pp. 53–133. https://doi.org/10.1016/s1546-5098(11)31002-3.

Guadagnolo, C.M., et al., 2001. Chronic effects of silver exposure on ion levels, survival, and silver distribution within developing rainbow trout (*Oncorhynchus mykiss*) embryos. Environ. Toxicol. Chem. 20, 553–560. https://doi.org/10.1002/etc.5620200314.

Gupta, Y.R., et al., 2016. Effect of copper nanoparticles exposure in the physiology of the common carp (*Cyprinus carpio*): biochemical, histological and proteomic approaches. Aquac. Fish. 1, 15–23. https://doi.org/10.1016/j.aaf.2016.09.003.

Handy, R.D., et al., 2002. Sodium-dependent copper uptake across epithelia: a review of rationale with experimental evidence from gill and intestine. Biochim Biophys. Acta 1566, 104–115. https://doi.org/10.1016/s0005-2736(02)00590-4.

Handy, R.D., 2003. Chronic effects of copper exposure versus endocrine toxicity: two sides of the same toxicological process. Comp. Biochem Physiol. A 135, 25–38. https://doi.org/10.1016/s1095-6433(03)00018-7.

Handy, R.D., et al., 2012. Ecotoxicity test methods for engineered nanomaterials: practical experiences and recommendations from the bench. Environ. Toxicol. Chem. 31, 15–31. https://doi.org/10.1002/etc.706.

Hoyle, I., et al., 2007. Dietary copper exposure in the African walking catfish, *Clarias gariepinus*: transient osmoregulatory disturbances and oxidative stress. Aquat. Toxicol. 83, 62–72. https://doi.org/10.1016/j.aquatox.2007.03.014.

Johnson, A., et al., 2007. The effects of copper on the morphological and functional development of zebrafish embryos. Aquat. Toxicol. 84, 431–438. https://doi.org/10.1016/j.aquatox.2007.07.003.

Keller, A.A., et al., 2013. Global life cycle releases of engineered nanomaterials. J. Nanopart. Res. 15, 1692. https://doi.org/10.1007/s11051-013-1692-4.

Kumari, P., et al., 2017. Mechanistic insight to ROS and apoptosis regulated cytotoxicity inferred by green synthesized CuO nanoparticles from *Calotropis gigantea* to embryonic zebrafish. Sci. Rep. 7, 16284. https://doi.org/10.1038/s41598-017-16581-1.

Lead, J.R., et al., 2018. Nanomaterials in the environment: behavior, fate, bioavailability, and effects-An updated review. Environ. Toxicol. Chem. 37, 2029–2063. https://doi.org/10.1002/etc.4147.

Li, J., et al., 1996. Kinetics of Cu^{2+} inhibition of Na^{+}/K^{+}-ATPase. Toxicol. Lett. 87, 31–38. https://doi.org/10.1016/0378-4274(96)03696-x.

Malhotra, N., et al., 2020. Review of copper and copper nanoparticle toxicity in fish. Nanomaterials 10, 1126. https://doi.org/10.3390/nano10061126.

McCormick, S.D., 1993. Methods for nonlethal gill biopsy and measurement of Na^{+}, K^{+}-ATPase activity. Can. J. Fish. Aquat. Sci. 50, 656–658. https://doi.org/10.1139/f93-075.

McKim, J.M., et al., 1978. Metal toxicity to embryos and larvae of eight species of freshwater fish-II: copper. Bull. Environ. Contam. Toxicol. 19, 608–616. https://doi.org/10.1007/BF01685847.

McNeil, P.L., et al., 2014. Effects of metal nanoparticles on the lateral line system and behaviour in early life stages of zebrafish (*Danio rerio*). Aquat. Toxicol. 152, 318–323. https://doi.org/10.1016/j.aquatox.2014.04.022.

McWilliams, P.G., Shephard, K.L., 1991. Water quality during egg incubation influences yolk-sac fry sodium kinetics in Atlantic salmon, *Salmo salar* L.: a possible mechanism of adaptation to acid waters. J. Fish. Biol. 39, 469–483. https://doi.org/10.1111/j.1095-8649.1991.tb04379.x.

Miller, T.G., Mackay, W.C., 1982. Relationship of secreted mucus to copper and acid toxicity in rainbow trout. Bull. Environ. Contam. Toxicol. 28, 68–74. https://doi.org/10.1007/BF01608415.

Muller, E.B., et al., 2015. Quantitative adverse outcome pathway analysis of hatching in zebrafish with CuO nanoparticles. Environ. Sci. Technol. 49, 11817–11824. https://doi.org/10.1021/acs.est.5b01837.

OECD, Test No. 236: Fish Embryo Acute Toxicity (FET) Test. Section 2. Organization for Economic Co-Operation and Development, Paris, 2013, pp. 22.

Ong, K.J., et al., 2014. Mechanistic insights into the effect of nanoparticles on zebrafish hatch. Nanotoxicology 8, 295–304. https://doi.org/10.3109/17435390.2013.778345.

Pelster, B., Bagatto, B., 2010. Respiration. In: Perry, S.F., et al. (Eds.), Zebrafish. Academic Press, London, pp. 289–309. https://doi.org/10.1016/s1546-5098(10)02907-9.

Peterson, R.H., Martin-Robichaud, D.J., 1986. Perivitelline and vitelline potentials inteleost eggs as influenced by ambient ionic-strength, natal salinity, andelectrode electrolyte; and the influence of these potentials on cadmiumdynamics within the egg. Can. J. Fish. Aquat. Sci. 43, 1445–1450. https://doi.org/10.1139/f86-177.

Ross, B.N., Knightes, C.D., 2022. Simulation of the environmental fate and transformation of nano copper oxide in a freshwater environment. ACS EST Water. https://doi.org/10.1021/acsestwater.2c00157.

Shaw, B.J., et al., 2012. Effects of waterborne copper nanoparticles and copper sulphate on rainbow trout, (*Oncorhynchus mykiss*): physiology and accumulation. Aquat. Toxicol. 116–117, 90–101. https://doi.org/10.1016/j.aquatox.2012.02.032.

Shaw, B.J., et al., 2016. A critical evaluation of the fish early-life stage toxicity test for engineered nanomaterials: experimental modifications and recommendations. Arch. Toxicol. 90, 2077–2107. https://doi.org/10.1007/s00204-016-1734-7.

Shaw, B.J., Handy, R.D., 2011. Physiological effects of nanoparticles on fish: a comparison of nanometals versus metal ions. Environ. Int. 37, 1083–1097. https://doi.org/10.1016/j.envint.2011.03.009.

Shephard, K.L., 1987. Ion-exchange phenomena regulate the environment of embryos in the eggs of freshwater fish. Comp. Biochem. Physiol. A 88, 659–662. https://doi.org/10.1016/0300-9629(87)90679-7.

Sun, Y., et al., 2016. Effects of copper oxide nanoparticles on developing zebrafish embryos and larvae. Int J. Nanomed. 11, 905–918. https://doi.org/10.2147/IJN.S100350.

Thit, A., et al., 2017. Effects of copper oxide nanoparticles and copper ions to zebrafish (*Danio rerio*) cells, embryos and fry. Toxicol. Vitr. 45, 89–100. https://doi.org/10.1016/j.tiv.2017.08.010.

van der Velden, J.A., et al., 1991. Early life stages of carp (*Cyprinus carpio* L.) depend on ambient magnesium for their development. J. Exp. Biol. 158, 431–438. https://doi.org/10.1242/jeb.158.1.431.

Vicario-Pares, U., et al., 2014. Comparative toxicity of metal oxide nanoparticles (CuO, ZnO and TiO_2) to developing zebrafish embryos. J. Nanopart. Res. 16, 2550. https://doi.org/10.1007/s11051-014-2550-8.

Wang, T., et al., 2014. The potential toxicity of copper nanoparticles and copper sulphate on juvenile *Epinephelus coioides*. Aquat. Toxicol. 152, 96–104. https://doi.org/10.1016/j.aquatox.2014.03.023.

Wang, T., et al., 2015. Effect of copper nanoparticles and copper sulphate on oxidation stress, cell apoptosis and immune responses in the intestines of juvenile *Epinephelus coioides*. Fish Shellfish Immunol. 44, 674–682. https://doi.org/10.1016/j.fsi.2015.03.030.

Zhang, Y., et al., 2018. Copper inhibits hatching of fish embryos via inducing reactive oxygen species and down-regulating Wnt signaling. Aquat. Toxicol. 205, 156–164. https://doi.org/10.1016/j.aquatox.2018.10.015.